P 56

Improving Lake-Effect Snow Forecasting through High Resolution MODIS Derived Ice Fields

Jonathan D.D. Meyer, Mark R. Hjelmfelt, and William J. Capehart

Institute of Atmospheric Sciences - South Dakota School of Mines and Technology

Abstract

Under fractional ice coverage conditions common to Lake Erie during the cold season, complex ice fields typically exist which are not accurately resolved under default settings in WRF. This project aims to improve the timing and location of Lake-Effect (LE) snow prediction over default conditions in WRF by using MODIS satellite imagery to derive high resolution ice fields to initialize WRF. Aircraft observations presented in Gerbush et al. (2008) showed that ice concentrations up to 70% had surface fluxes consistent with open water values. Threshold classification methods used in NWP for the determination of ice cover potentially causes under-estimation of surface fluxes of sensible heat (SH) and latent heat (LH) during conditions of partial ice cover; both of these fluxes play an integral role in the LE process. These results lead to the conclusion that operational models using thresholds of ~50% ice cover to dictate open-water/ice covered grid cell classification could likely misrepresent a complex ice field and therefore the surface flux fields.

Initial results using high resolution ice field initialization in WRFV3.0 and WRFV3.1 show substantial deviations in mesoscale variables responsible for LE development compared to control runs using default settings; this suggests initialization of WRF using high resolution ice fields can influence LE forecasting.

1. INTRODUCTION

Lake Effect (LE) snow storms have the potential of creating substantial challenges to communities and regional government agencies in the lee of the Great Lakes. Extreme accumulations of snow are possible from destabilization of the air masses as they pass over open water. Adding to the high impact the storms themselves have on communities, forecasting of LE storms has presented challenges to operational forecasters. The large environmental sensitivities of the timing and location of LE storms create large uncertainties in weather forecast models. These forecast models are heavily relied upon for both short and long term weather forecasts by operational forecast offices such as the National Weather Service (NWS). When uncertainties exist in the model guidance, decision making at the local and regional level can become difficult and can often lead to incorrect deployment of resources, further stressing local economies. Ice cover over the Great Lakes presents special difficulties for models. This study examines WRF forecast issues and improvements using high resolution satellite observations as initialization.

Recent research by Gerbush et al. (2008) measured the effect of fractional ice fields over Lake Erie on the exchange of surface fluxes of sensible and latent heat (SH and LH). They showed that both research models such as the Weather Research and Forecasting (WRF) model (Skamarock et al., 2008) and operational forecasting models, i.e., Global Forecasting System (GFS) and the North American Model (NAM), are potentially misrepresenting the surface flux fields over fractional ice cover. Gerbush et al. showed through aircraft measurements that both SH and LH over fractional ice fields remained nearly consistent with open water values up to approximately 70% ice cover. SH decreased non-linearly above 70% while LH decreased linearly above 70%. Observations were acquired during the Great Lakes Ice Cover and Atmospheric Flux (GLICAF) experiment by the University of Wyoming's King Air aircraft which flew flight tracks over sections of Lake Erie at heights of 45 and 500-m above the lake surface. Figure 1 shows the results from Gerbush et al. (2008) taken from the 45-m high flight track and shows the best-fit linear (LH) and non-linear (SH) regression lines for 45-s averaged data points.

* *Corresponding author address:* Jonathan Meyer, Institute of Atmospheric Science, SD School of Mines, Rapid City, SD 57701-3995; e-mail: jonathan.meyer@mines.sdsmt.edu.

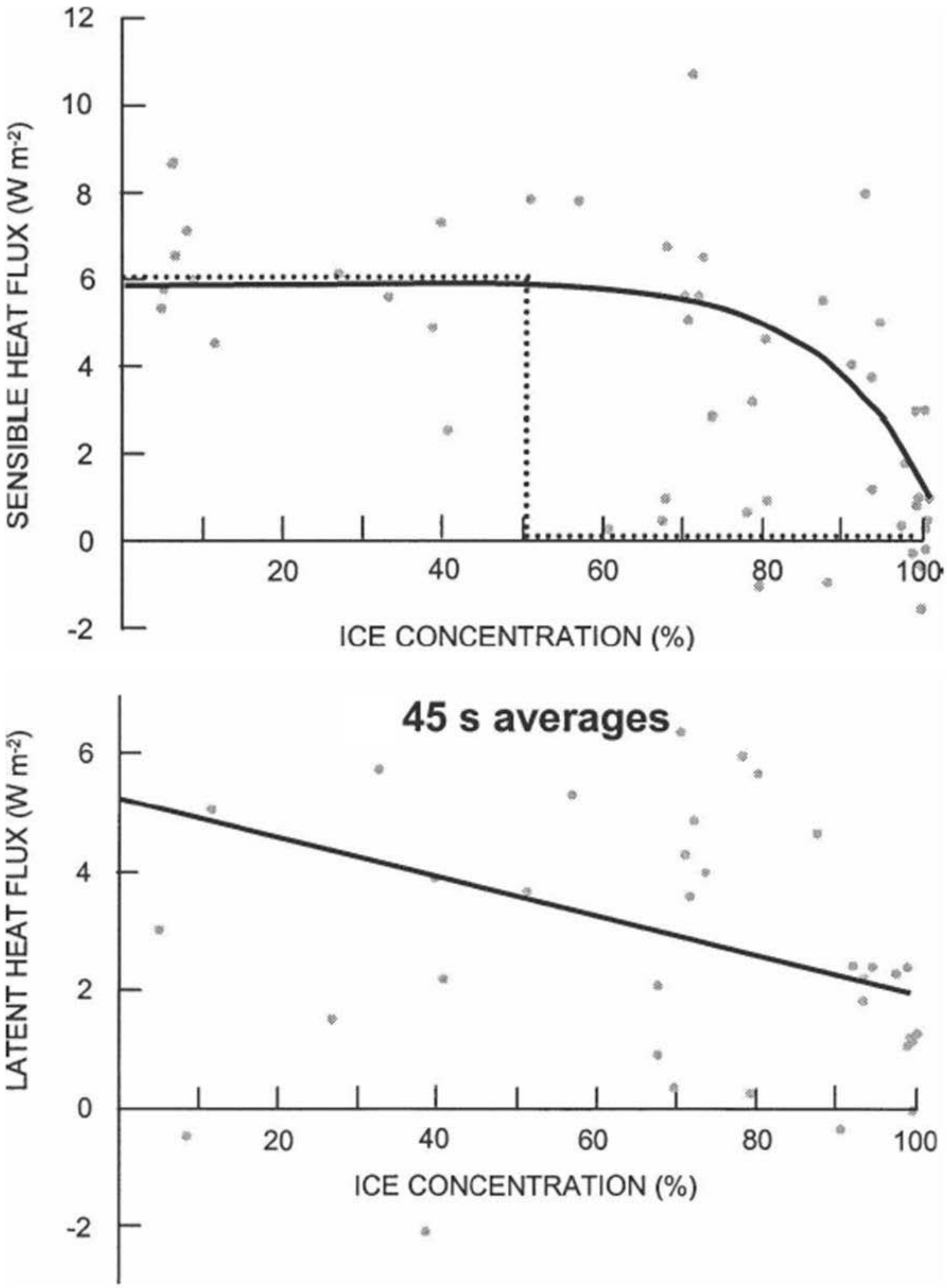

Figure 1: 45 s averaged sensible and latent heat fluxes compared to ice concentration percentage observed for the 45-meter flight tracks. Best-fit non-linear (SH flux) and linear (LH flux) regression lines are shown for each example. The dotted black line represents the typical representation of fluxes and ice concentrations in NWP models (as seen in Fig. 2). Adapted from Gerbush et al. (2008)

The aforementioned research and operational NWP models such as the GFS, NAM, and WRF-ARW currently employ a water grid cell classification method that uses a threshold value of ice concentration to determine if the grid cell is open water or ice covered with no fractional ice coverage allowed. The threshold value varies depending on the particular model but typically fluctuates around 50%. Using threshold values of ~50% can potentially misrepresent the true exchange of both SH and LH from the surface of the water body. Grid cells containing ice cover from the threshold up to ~70% ice cover can be erroneously classified as completely ice-covered whereas the actual exchange of fluxes are closer to open water values. As the exchange of both SH and LH are primary mechanisms for the destabilization of the boundary layer and thus LE convection, misrepresentation of these flux fields inevitably introduces additional uncertainties into the model output. Figure 2 shows the fractional sea ice concentration compared with SH and LH from the WRF model simulations, and summarizes the effect that the threshold method has on the amount of fluxes exchanged from the surface into the atmosphere.

Converting the sea-ice field from either the default North American Regional Reanalysis (NARR, Mesinger et al., 2006) or high resolution ice-cover data (discussed in greater detail in section 2) to the model domain grid is performed by the METGRID.EXE program. METGRID.EXE creates NetCDF files (met_em) that contain fractional ice values for the grid points classified as water. These met_em files are then read by program REAL.EXE which interpolates the data vertically onto the model coordinates. During REAL.EXE, fractional ice values ranging from between 0 to 1(0 = open water, 1 = ice cover) are converted to a 'binary' value (sea-ice field only contains 0, for open water or 1, for ice covered) where the threshold method determines if the grid cell is either open water or ice covered. In the case of WRF_V3.1, the threshold is shown as 50% where any fractional amount of ice above 50% forces the grid cell to be treated as ice-covered, minimizing the amount of fluxes calculated by the Land Surface Model (LSM, after Chen and Dudia (2001)). The wide variance for SH flux over low ice concentrations shown in Fig. 2 is a result of the LSM's dependency on sea surface temperatures (SST) to calculate the fluxes over open water grid cells. Grid cells classified as ice-covered remain near zero SH exchange due to typical colder temperatures and the removal of the temperature gradient forcing of heat flux.

This project tests the sensitivity of numerical weather prediction (NWP) models to fractional ice cover and its influence on surface heat fluxes such as sensible (SH) and latent heat (LH) and LE snow. Comparisons between the Weather and Research Forecasting Advance Research WRF model (WRF-ARW) and both observed LE events and *in situ* measurements over fractional ice-covered Lake Erie will be presented. Increasing the accuracy of surface flux fields should decrease the uncertainties of NWP related to timing and location of LE snow. Ideally, increasing the accuracy of the surface flux fields will increase the lead times that operational forecasters can issue confident forecasts of impending LE snow events.

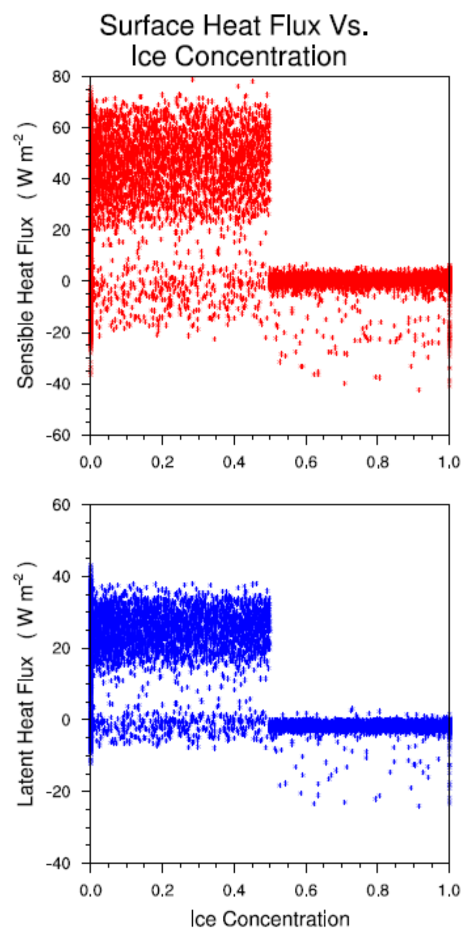

Figure 2: Sensible (upper) and Latent (lower) heat flux (W/m^2) and Ice Flag concentration. Taken from WRFV3.1 for the February 2004 non-LE case initialized with MODIS satellite derived high-resolution ice fields.

2. CASE STUDIES AND METHODS

The goal of this study is to improve the accuracy of Great Lake ice fields; this is done using Moderate Resolution Imaging Spectroradiometer (MODIS) satellite images coupled with Great Lakes Environmental Research Laboratory (GLERL) sea-ice and SST analysis in place of the default SST and Sea Ice values provided by first guess fields from continental-scale forecast models. The high-resolution ice fields and GLERL fields yield the most representative ice and SST fields available, and provide WRF's LSM model with the most accurate grid cell depiction of factors influencing the LE process.

This research focuses on two case studies involving air flow over the Great Lakes with large areas of ice cover and utilizes both WRF Version 3.0 and WRF Version 3.1 to compare observed data with model output. The first case study is based on material in Gerbush et al. (2008) (henceforth referred to as the Gerbush Case). WRF model simulations for the Gerbush case are run for 36 hours beginning on 25 February 2004 at 12:00 UTC and ending on 27 February 00:00 UTC. The second case study is an event previously described by Cordeira and Laird (2008) (henceforth referred to as the Cordeira Case).The Cordeira and Laird study focused on the ability of ice cover to effectively enhance LE processes when coupled with particular mesoscale and synoptic conditions. WRF simulations for the Cordeira case study were run from 9 February 2003 at 00:00 UTC to 15 February at 00:00 UTC.

2.1 Mesoscale model

WRF-ARW was selected for this study due to its variety of physics options and ability to perform high resolution simulations. Also, WRF-ARW's pre-processing routines have the ability to deal with multiple initialization fields and missing data values; this is invaluable when dealing with large domains and smaller high resolution data sets (i.e. fractional ice fields over the Great Lakes). The model domains are shown in Fig. 3. A coarse grid domain (D01) was centered at 40.9° N and 94.1° W, with 200 x 100 horizontal grid points with 30 km grid spacing. Nesting domains at a 3:1 ratio gives the following domain characteristics: domain 2 (10 km, 238 x 175), domain 3 (3.33 km, 235 x 205), domain 4 (1.11 km, 412 x 289) and domain 5 (0.37 km, 493 x 430). For each modeled situation, at least 3 domains are run with some using 4 and others 5 domains as shown in Table 1. The 5th domain is only employed for the Gerbush case study where extremely high resolution of 370-m is necessary to resolve the 45-m vertical height measurements of heat flux values compared with ice concentrations. For the Cordeira cases, the 3- and 4-domain simulations are used to test whether an increase in horizontal resolution leads to an improvement of the timing and location of LE snow by improving the ice field representations. Outer domain time steps for each model were 90-s and the model employed a Lambert Conformal Conic map projection.

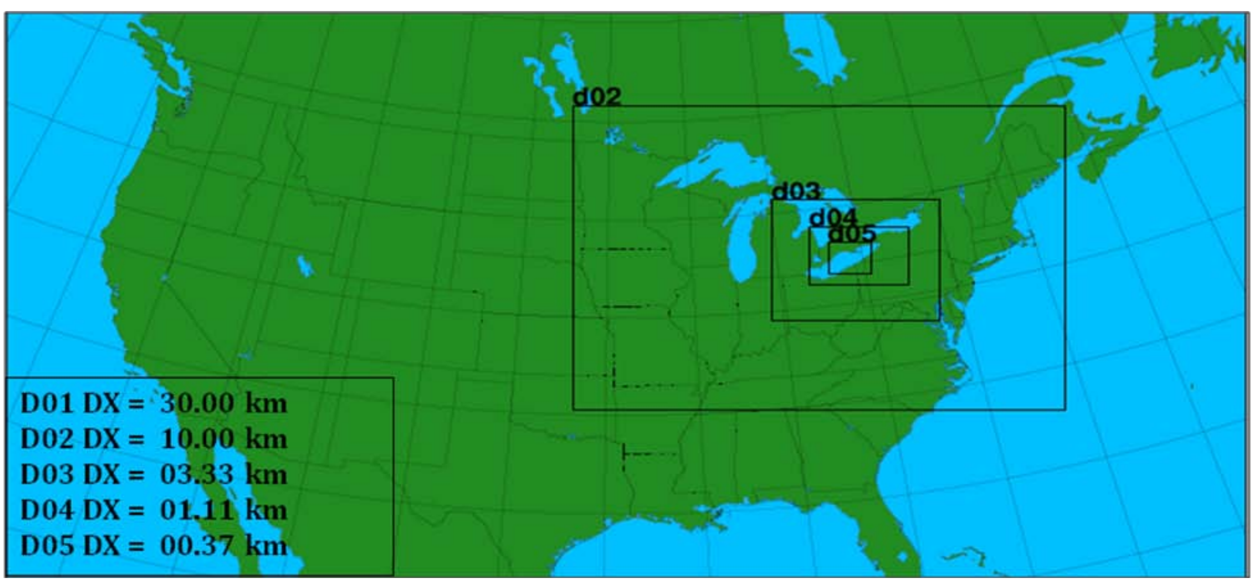

Figure 3: Domains 1 – 5 nesting down over the Great Lakes region and Lake Erie as well as their horizontal resolutions.

Table 1: Outline showing suite of WRF model runs and the physics options for the WRF simulations employed for those WRF runs.

Case	Model	Version	3domain	4domain	5domain	
Feb2003	WRFV30	default	X	X		Feb2003_WRFV30_control
	WRFV310	default	X	X		Feb2003_WRFV310_control
	WRFV310	icefree	X	X		Feb2003_WRFV310_icefree
	WRFV310	highres	X	X		Feb2003_WRFV310_highres
	WRFV310	polarwrf	X	X		Feb2003_WRFV310_plrwrf
Jan2004	WRFV30	default	X			Jan2004_WRFV30_control
	WRFV310	default	X	X		Jan2004_WRFV310_control
	WRFV310	icefree	X	X		Jan2004_WRFV310_icefree
	WRFV310	highres	X	X		Jan2004_WRFV310_highres
	WRFV310	polarwrf	X	X		Jan2004_WRFV310_plrwrf
Feb2004	WRFV30	default	X			Feb2004_WRFV30_control
	WRFV310	default	X	X	X	Feb2004_WRFV310_control
	WRFV310	icefree	X	X	X	Feb2004_WRFV310_icefree
	WRFV310	highres	X	X	X	Feb2004_WRFV310_highres
	WRFV310	polarwrf	X	X	X	Feb2004_WRFV310_plrwrf

Model Physics Option	
MicroPhysics	Thompson graupel scheme (2-moment scheme in V3.1)
Longwave Radiation	Rapid Radiative Transfer Model (RRTM)
Shortwave Radiation	Dudhia scheme
Surface Layer Physics	Monin-Obukhov (Janjic Eta) scheme
Land Surface Model	unified Noah land-surface model
Planetary Boundary Layer	Mellor-Yamada-Janjic (Eta) TKE scheme
Cumulus Physics	Grell-Devenyi ensemble scheme

Terrain data sets were obtained through the United States Geological Survey (USGS) with resolutions of 5 minutes for D01, 2 minutes for D02, and 30 seconds for D03 – D05. The model employed the NOAH LSM which predicts soil moisture, temperature at 4 depths, canopy moisture, and snow depth (Chen and Dudhia, 2001a,b). The model was initialized with NARR data sets. The model employs 43 vertical levels where approximately 20-25 layers occur in the lower 200 hPa to fully resolve the lower boundary layer processes responsible for LE snow. The upper boundary of the simulations is 100 hPa.

Lake surface temperatures were obtained from the GLERL data. GLERL SST fields were employed for the ice-free simulations and the high resolution ice simulations, while default NARR SST fields were used for the control cases.

Inputs such as the GLERL SSTs and the MODIS-derived high resolution ice fields were fed into the model framework so that the higher resolution fields were laid on top of fields with lower resolution. The order in which the fields were applied was 2D and 3D NARR meteorological fields first, followed by NARR surface fields, and finally the high resolution GLERL SSTs and MODIS-derived ice fields. The ice fields and SSTs are held constant for the duration of each model simulation. Selection of the appropriate MODIS satellite image was based on the timing of the observed LE snow and availability and quality of the MODIS satellite image to ensure that the ice field input into WRF was representative of the actual ice field influencing the LE process.

For each of the case studies, a suite of WRF models was developed to test the effectiveness of changes dealing with the treatment of fractional ice cover and the calculation of surface fluxes. WRF_V3.1 was released during the developmental phase of this research and will be the main model of choice for comparisons, although WRF_V3.0 was run using default conditions. Table 1 outlines the various WRF models run and their common designation along with the model physics options employed for all WRF simulations. In addition to the default runs, which automatically classified a majority of Lake Erie with unrealistic amounts of ice cover, an ice-free case was run where the sea-ice threshold option in WRF_V3.1 was set to a value low enough to ensure that all water grid cells would not contain ice. By doing this, SSTs are able to dictate flux exchanges over a water body. Figure 4 shows SST values for each of the WRF model runs for the Gerbush case and indicates the low SST values covering Lake Erie for the ice-free case using default SSTs. These cold values suppress the realistic open water heat fluxes and produce results similar to the ice covered default settings.

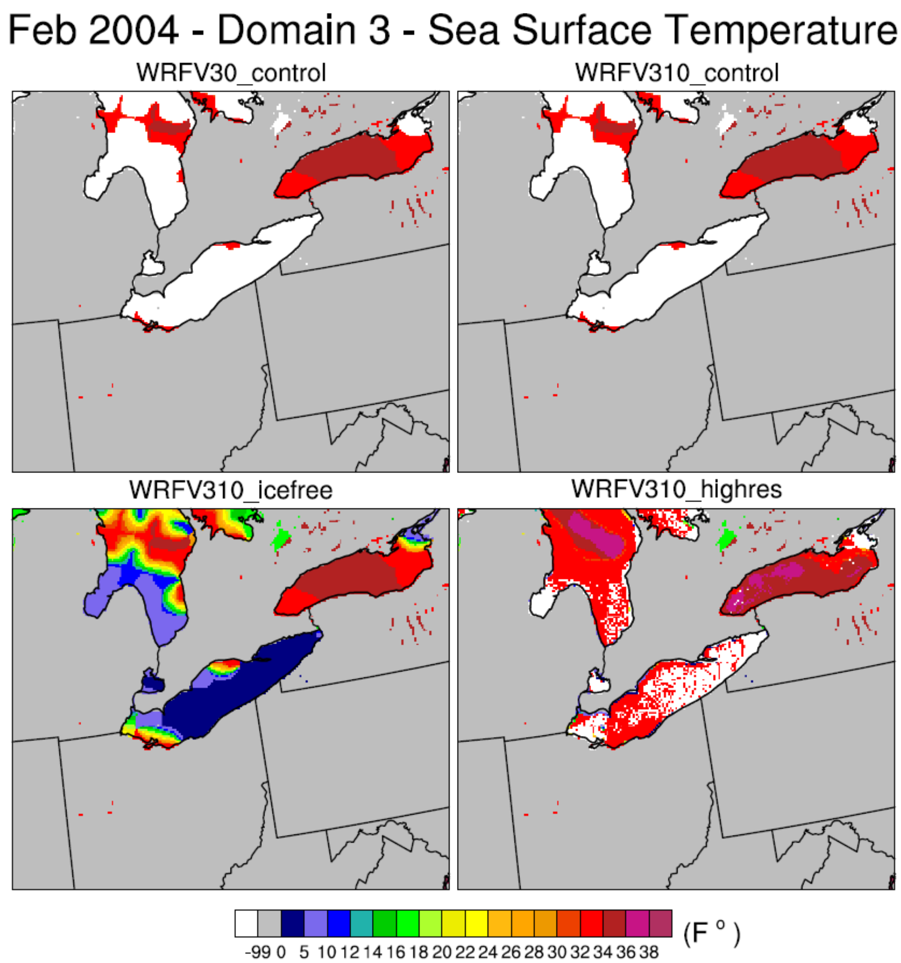

Figure 4: Gerbush case SST values shown in color-filled contours where Grey represents land surface, and White represents ice cover. Note the unrealistic cold values for the WRFV310_icefree case for 'water' points. These values will eventually be replaced with GLERL SSTs shown underneath the high-resolution ice fields in the WRFV310_highres case.

A second set of the ‘ice-free’ runs utilize the same GLERL analyzed SSTs for the WRF high-resolution ice (WRFV310_highres) cases; this allows a more realistic SST field with values hovering just above the freezing point. Results from the GLERL SST-driven ice-free cases will be presented in the results section while the default SST ice-free cases are noted as a problem in setting the sea-ice threshold to force an ice-free case. The corrected ice-free case showcases the maximum available exchange of surface fluxes and tests the environmental sensitivity to the ice fields.

The most recent version of WRF, Version 3.1, includes a new fractional sea-ice option. This option was developed by the Polar WRF group and improves on the calculation of surface fluxes over complex ice cover (Hines and Bromwich, 2008; Bromwich et al., 2009). The fractional sea-ice option calculates the fluxes for a grid cell based on a weighted average for the concentration of ice. The LSM is called for both open water and ice-covered calculations and weights each value based on the concentration of ice. Using the fractional sea-ice option creates a more realistic value of the fluxes for that grid cell and removes the reliance on the threshold method mentioned previously. While this option is considered an improvement over previous methods, using the fractional ice option will create a linear relationship between ice cover and SH, which remains problematic in light of the findings by Gerbush et al. (2008) suggesting a non-linear trend with little deviation from open water values up to ~70% ice cover. While the fractional ice option works well for LH fluxes which were shown by Gerbush et al. to follow a linear trend, a patch for the fractional sea-ice option may be necessary to accurately representing SH fluxes over fractional ice cover.

2.2 Case Studies

The Gerbush case compares model simulations to measurements of SH and LH fluxes collected by the University of Wyoming’s King Air aircraft during the GLICAF field campaign. Figure 5 shows the sea-ice field for the various WRF simulations of the Gerbush case in February 2004. Figure 6 shows the MODIS satellite image taken over Lake Erie on 1815 UTC 26 February 2004. This MODIS satellite image was used to derive the high resolution sea-ice fields for the Gerbush case. Ice field charac-teristics such as fast ice (semi-permanent ice), leads (cracks and splits of varying size with exposed open water), and complex ice (newly forming and drifting ice fields with frequent transitions between ice cover and open water) are indicate. These features are accurately resolved in the domain 4 WRFV31 highres simulation shown in Fig. 7. The Gerbush case is a non-LE snow case and model output is compared to measurements in an attempt to replicate the observed relationships between ice cover concentrations and the respective surface flux fields.

The Cordeira case study was chosen due to slight-to-moderate LE snow that was observed to occur over a highly ice-covered Lake Erie. Figure 8 shows analysis of snowfall totals during the Cordeira LE event. Lake Ontario, which remains mostly ice-free, exhibits the potential of the LE process while Lake Erie, which contained large concentrations of ice, shows limited snow fall accumulations. Snowfall accumulations downwind of Lake Erie shown in Fig. 8 were not anticipated due to the large concentrations of ice over Lake Erie and were not well predicted by forecast models in the days leading up to the LE events (Cordeira and Laird, 2008). Simulations for the Cordeira case will be compared to observed values of snowfall accumulations in an attempt to better recreate the timing and location of observed LE snowfall.

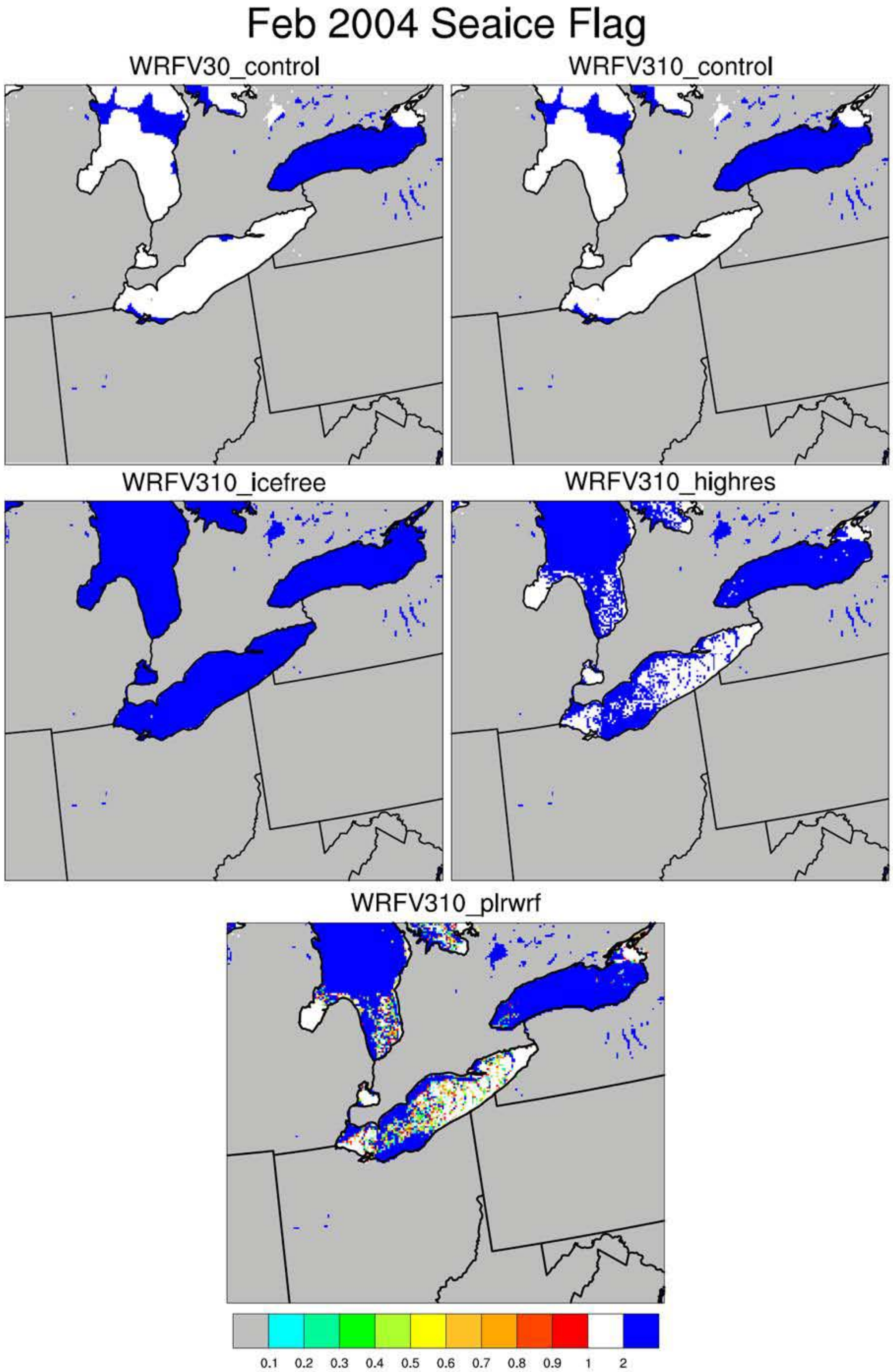

Figure 5: Domain 3 sea_ice field from each WRF model permutation. The top 4 plots represent WRF's sea_ice flag using either open water (Blue) or ice cover (White); WRFV310_plrwrf (bottom panel) employs the fractional-sea_ice option in V3.1 and represents the fractional field from 0 (open water) to 1 (ice-covered).

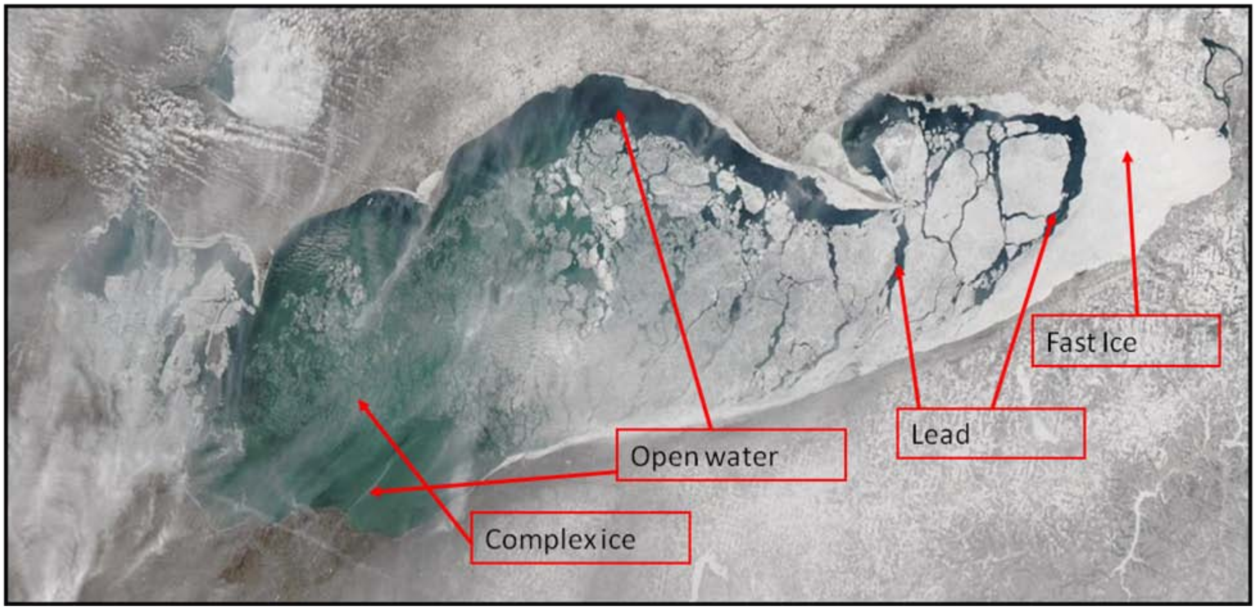

Figure 6: MODIS satellite image taken over Lake Erie on 18:15 UTC 26 February 2004. Ice field characteristics such as fast ice (stationary thick ice), leads (cracks and splits of varying size of open water between ice sheets), and complex ice (newly forming and drifting ice fields with frequent transitions between ice cover and open water) are indicated.

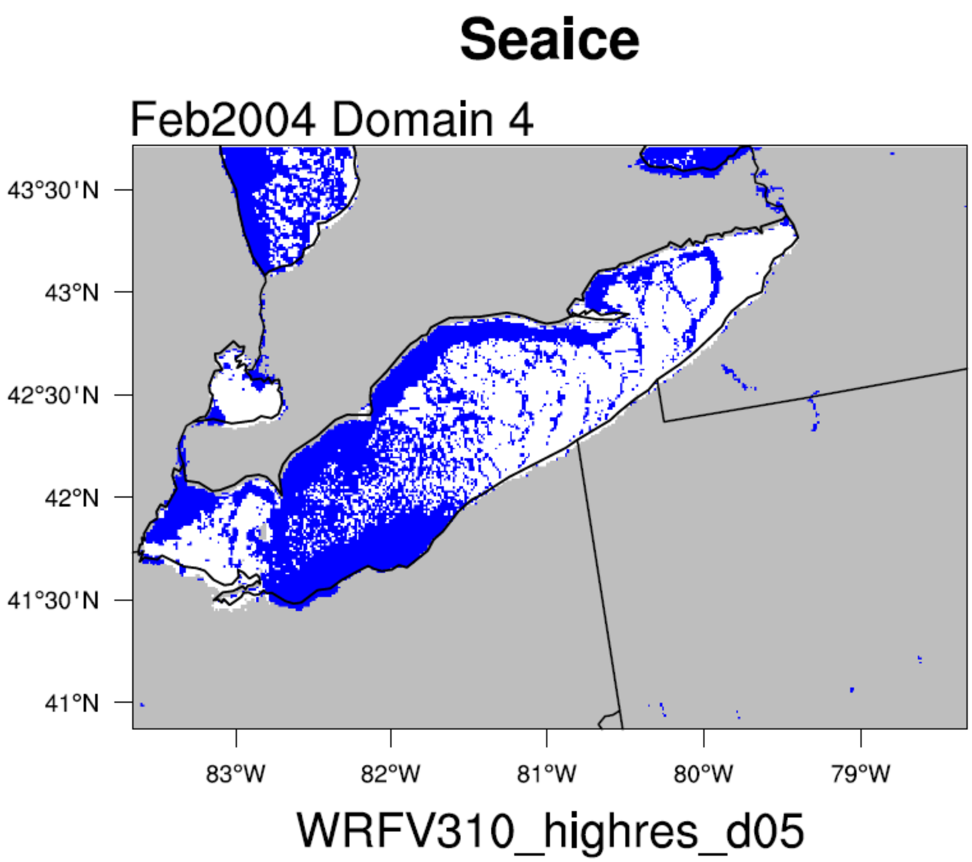

Figure 7: Domain 4 Sea_ice from WRFV310 high resolution 5 domain simulation (White = Ice, Blue = Water, Grey = Land).

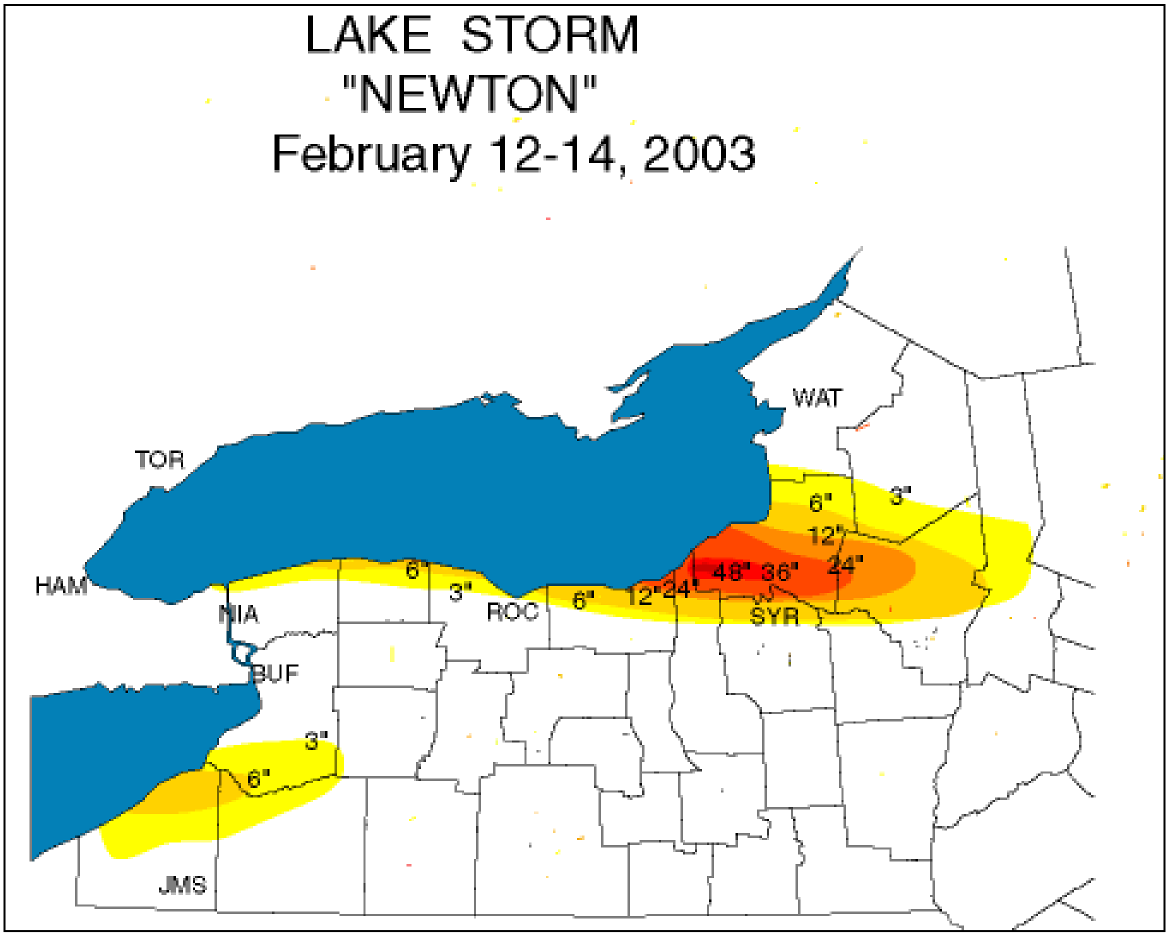

Figure 8: NWS snowfall totals for February 2003 Cordeira LE case centered over Lake Ontario Obtained from the National Weather Service, Buffalo, New York Office's Lake Effect page (http://www.erh.noaa.gov/buf/lakeeffect/lake0304/i/stormi.html)

3. RESULTS

Results will be presented for the Gerbush case comparing the high resolution ice simulations and the default simulations as well as brief comparisons between the ice-free and the default simulations for the February 2003 Cordeira simulation.

3.1 Gerbush Case Study Results

As noted earlier, the Gerbush case study is a non-LE case with no precipitation. The influences of fractional ice cover on both the exchange of surface heat fluxes and the modification of mesoscale circulations that can influence LE snow can be substantial. Default initializations from NARR have been shown to be heavily biased towards complete ice cover over Lake Erie when actual concentrations can be significantly less (e.g. Fig. 5 and Fig. 6).

Figure 9 shows 2-m air temperature and 10-m wind vectors and illustrates the difference between the control case and the high resolution ice case under daytime high wind conditions. During this output period, temperature advection over Lake Erie mixes out any local gradients existing in air immediately above ice cover and open water. Despite little variance in temperature surrounding the Great Lakes, the difference plot (lower panel) shows strong temperature increases downwind of Lake Erie due to temperature advection over Lake Erie. This warm advection pattern can exert important influences on the Convective Boundary Layer and LE snow accumulations just offshore of Lake Erie.

In addition to ice cover influences on temperature variations, influence on surface moisture availability and transport plays a role in LE accumulations. Figure 10 shows 2-m moisture and 10-m wind vectors, and illustrates processes similar to those described for Fig. 9. As was evident in Fig. 9, the higher winds in Fig. 10 mix out the localized gradients created by the complex ice cover while advecting the higher moisture values downwind of Lake Erie.

One of the most perceptible influences of the treatment of ice cover on processes in NWP applications is its impact on surface heat fluxes. As mentioned above, NWP threshold methods used to differentiate between open water and ice-covered grid cells have a high potential to erroneously classify fractionally ice-covered grid cells. Fractionally ice-covered grid cells likely exhibit values of surface heat flux similar to open water values but are frequently declared ice-covered, capping any exchange of surface heat fluxes.

When analyzing heat flux fields it became apparent that the land mask being used to define LSM fields had an insufficient resolution and caused erroneous calculations of the heat flux fields in regions surrounding the Great Lakes. Default settings utilize the land mask named LANDSEA, one of two land-sea masks in the WRF framework, with this one representing the land-sea mask for the meteorological fields used to initialize WRF. The second land mask, LANDMASK, represents the final land-sea mask of the simulated domain. Typically, for course resolutions the default settings are adequate, but when nesting down under 3 kilometers, the coarser resolution of the LANDSEA field compared to LANDMASK can create water/land grid cells that overlap onto their opposing type of land cover. Figure 11 shows the difference in LANDMASK and LANDSEA and illustrates the overlapping of grid cells over the shores of Lake Erie in the LANDSEA plot but not in the LANDMASK plot.

Comparison of SH between the high-resolution simulation and the control simulation is shown in Fig. 12. Largest values of SH flux are shown to occur over the central region which contains complex ice and open water. The difference plot (lower panel) indicates a bias over Lake Erie with higher values of SH for the high resolution ice case while regions downwind of Lake Erie show negative values, indicating that the control WRF run contained larger values of SH flux than the high-resolution case due in part to the presence of cloud cover in the control simulation. Calculation of SH over water surfaces are driven by the SSTs (along with several other atmospheric factors) such that warmer SSTs lead to higher upward heat flux. Analysis of LH fields presented comparable features as Fig. 12 due to similar controlling factors.

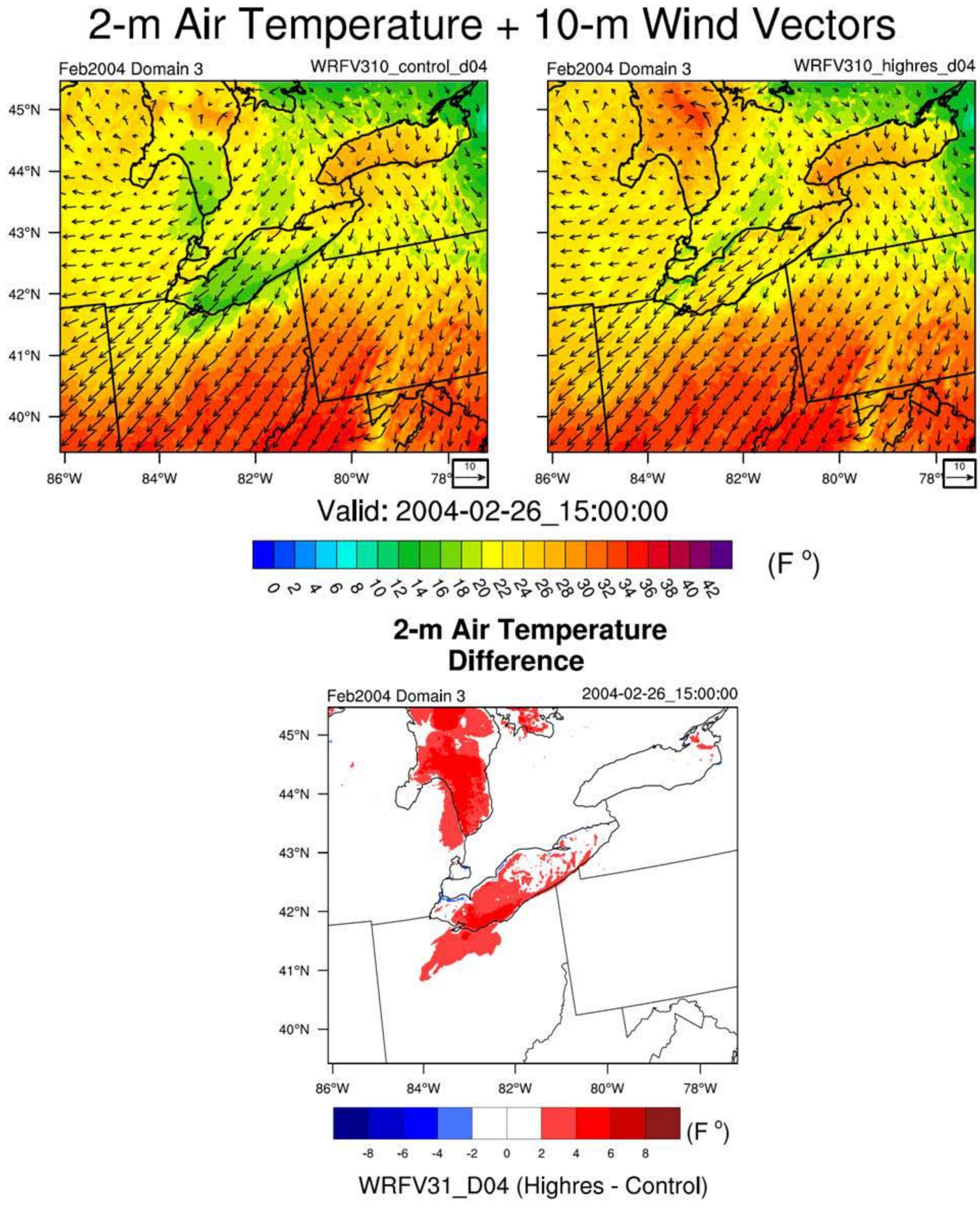

Figure 9: 3-panel plot showing 2-m air temperature (F) and 10-m wind vectors of the WRFV31_control (upper left) and WRFV31_highres (upper right) cases for 15:00 UTC, 26 February, 2004. The lower plot represents the difference between the Highres case and the Control case where positive (red colors) represent the Highres case having warmer temperatures than the Control case and negative (blue colors) represent cooler temperatures for the Highres case.

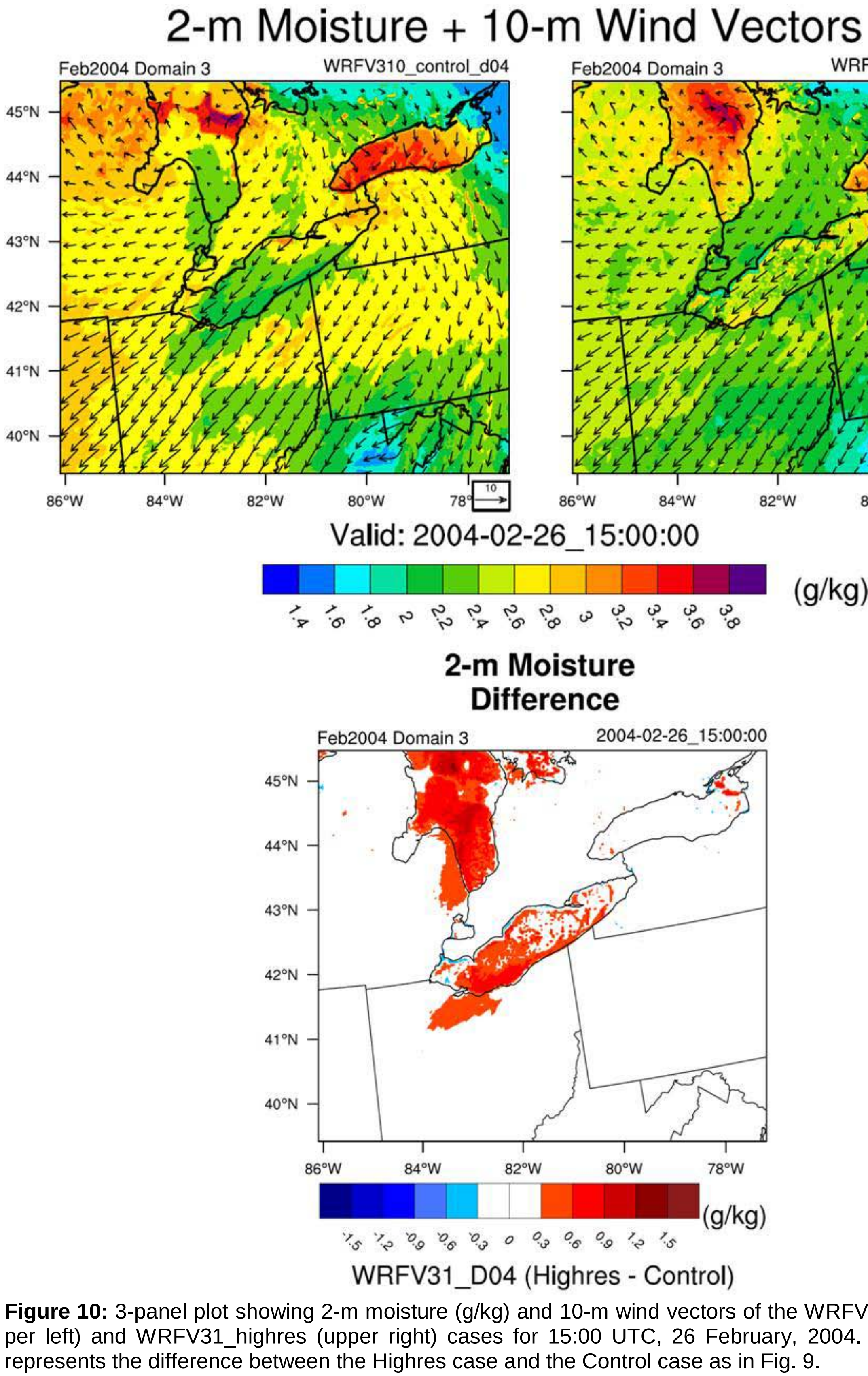

Figure 10: 3-panel plot showing 2-m moisture (g/kg) and 10-m wind vectors of the WRFV31_control (upper left) and WRFV31_highres (upper right) cases for 15:00 UTC, 26 February, 2004. The lower plot represents the difference between the Highres case and the Control case as in Fig. 9.

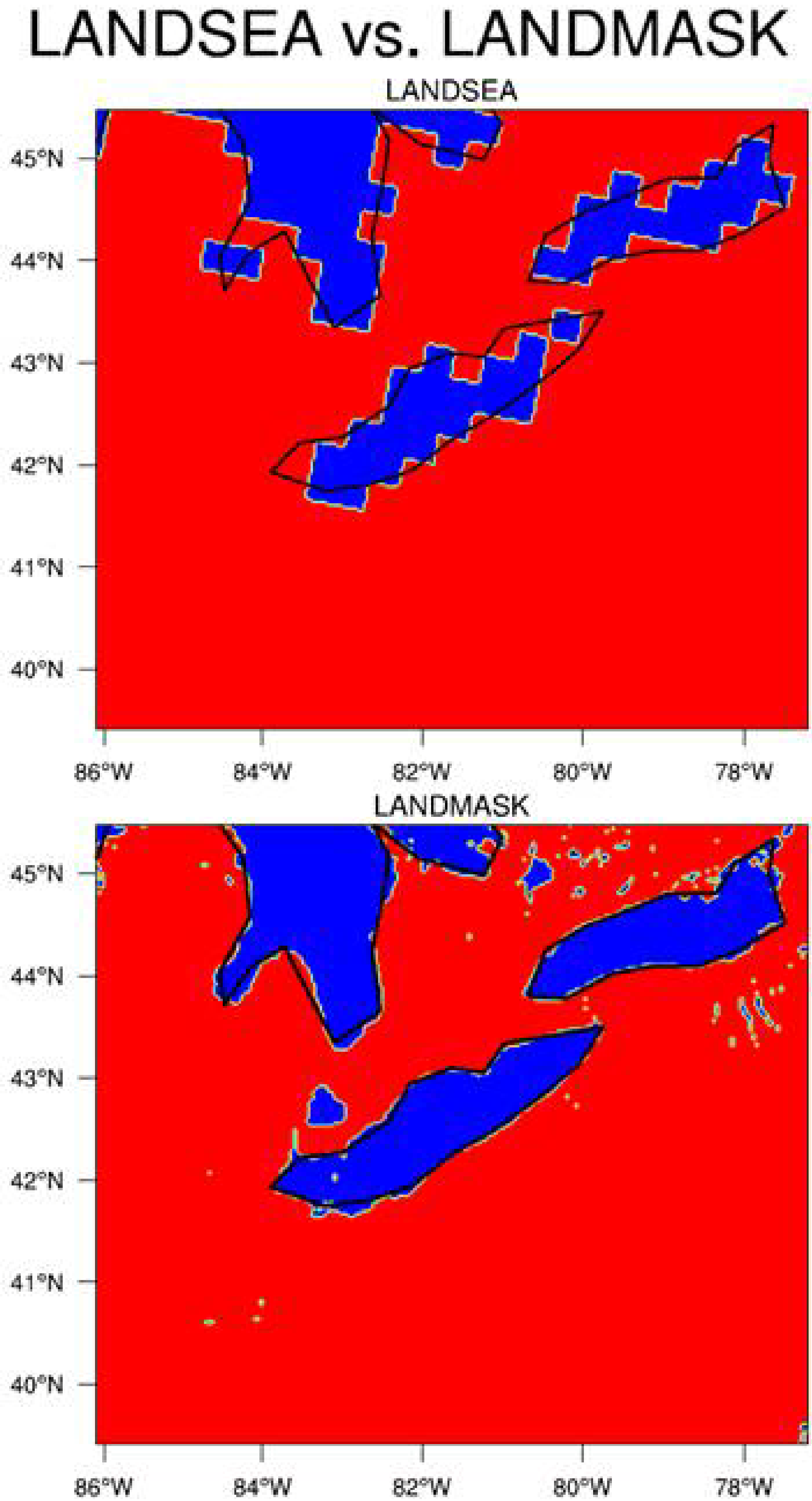

Figure 11: 2-panel plot comparing the LANDSEA field (upper) and the LANDMASK field (lower) illustrating the overlapping of water/land grid cells for the LANDSEA field while the LANDMASK field retains the Great Lakes borders with a higher degree of accuracy. Red represents land cover while blue represents water.

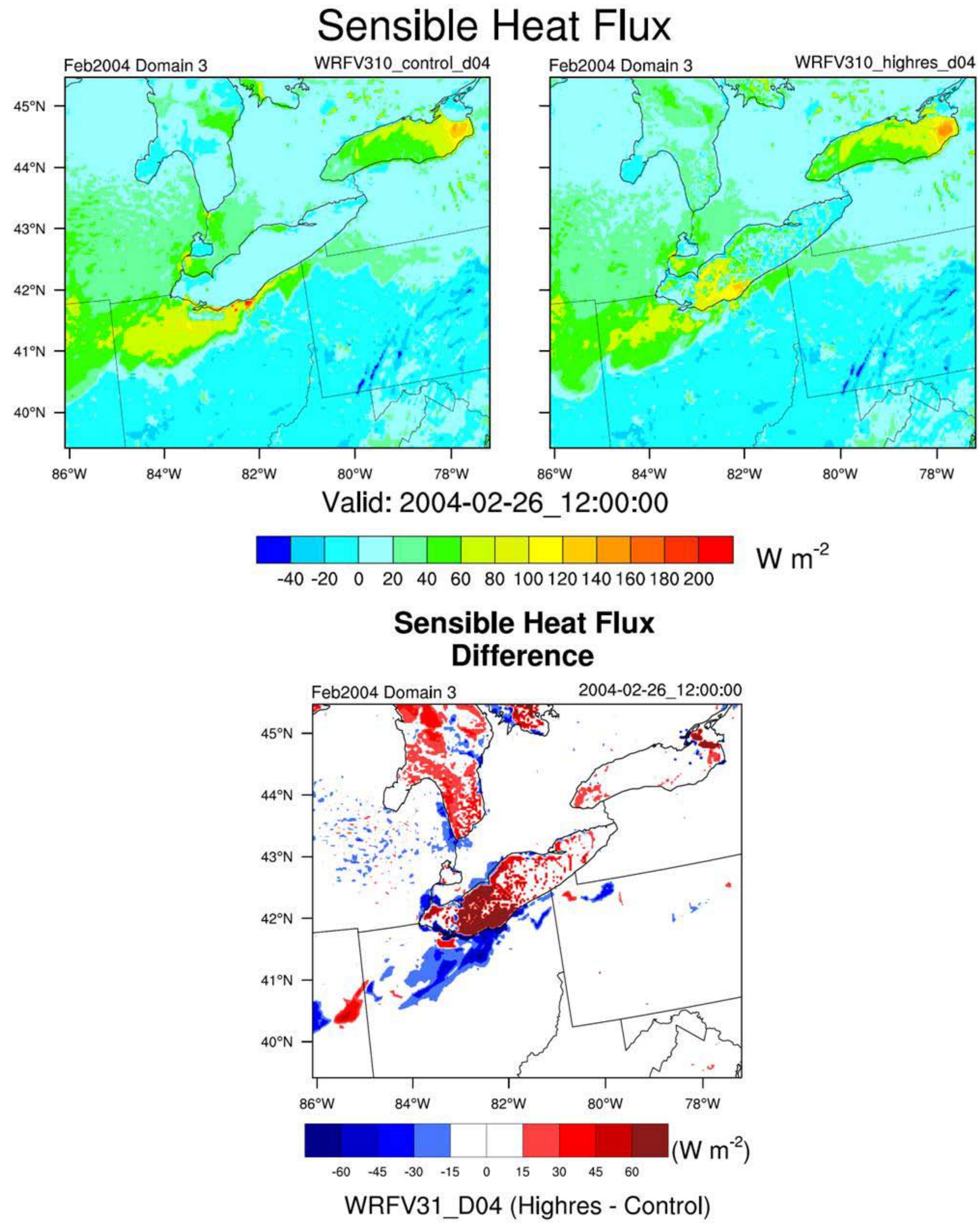

Figure 12: 3-panel plot comparing the WRFV31_control (upper left) and the WRFV31_highres (upper right) output for sensible heat flux (HFX- W/m^2) for the Gerbush case for 12:00 UTC, 26 February, 2004. The difference between the highres case and the control case is illustrated in the lower panel as in Fig. 9.

3.2 Cordeira case study results

This section will present initial results from the Cordeira February 2003 case study (aka Lake Storm Newton). As shown in Fig. 8, Lake Storm Newton had snow accumulations of 3-6 inches on the northeastern shores of Lake Erie south of Buffalo, New York. These snow accumulations were modest compared to the accumulations seen on the southeastern shores of Lake Ontario but were not anticipated in forecast model output. Figure 13 compares model total snow depth for the WRF_V31 control (top left) vs. the WRF_V31 ice-free case (top right) with a difference plot of the ice-free case subtracted from the control case (lower panel). For the control case, slight accumulations are shown to occur for regions downwind of Lake Erie but for the most part, accumulations are minimal. On the other hand, the ice-free case resulted in large accumulations upwards of 25 inches downwind of Lake Erie. There is excellent agreement in the placement of the largest accumulations between the NWS's analysis shown in Fig. 8 and the model result shown in Fig 13.

Maximum accumulations for the ice-free case occurred roughly between 18:00 UTC, 12 February, 2003 – 18:00 UTC on 13 February. Results from this case study will focus on 06:00 UTC, 13 February 2003 when the processes controlling the LE process were most predominant, highlighting the differences between the control and the ice-free cases.

As seen earlier for the Gerbush case, 2-m air temperature and moisture along with 10-m wind vectors can illustrate the influence of the lake body on the boundary layer leading to enhancement of LE processes. Figure 14 shows the 2-m air temperature with 10-m wind vectors for the WRF_V31 control (upper left) and the ice-free case (upper right), with the lower panel showing the difference between the two. This image illustrates the significantly warmer temperatures over the ice-free lake surface as exchange of SH is able to warm the over-riding air. This is especially apparent for the northeastern basin of Lake Erie where temperatures exceed the control case by 8 degrees Fahrenheit. This increase in air temperature, due to the exchange of SH from the lake surface, destabilizes the CBL and leads to enhanced vertical motion of the over-riding air, and higher accumulations of snowfall. The difference plot (lower panel) effectively shows the enhancement of the 2-m air temperatures downwind of all the major Great Lakes. Also of interest for the ice-free case is the presence of a convergence zone downwind of Lake Erie located over northeastern Ohio and northwestern Pennsylvania. This convergence zone indicates the influence temperature gradients caused by exchange of SH can have on the mesoscale circulations surrounding large bodies of water.

Comparisons for the LH field are revealed in Fig. 15, which show the WRF_V31 control and ice-free cases with the lower panel representing the difference between the two cases. LH fluxes over the Great Lakes are substantially increased over the control case for ice-covered portions of the Great Lakes and completely ice-covered Lake Erie. SH fields presented similar features as LH in Fig. 15. The large SH and LH flux values over the Great Lakes for the ice-free case enhanced the LE event leading to the high snowfall accumulations.

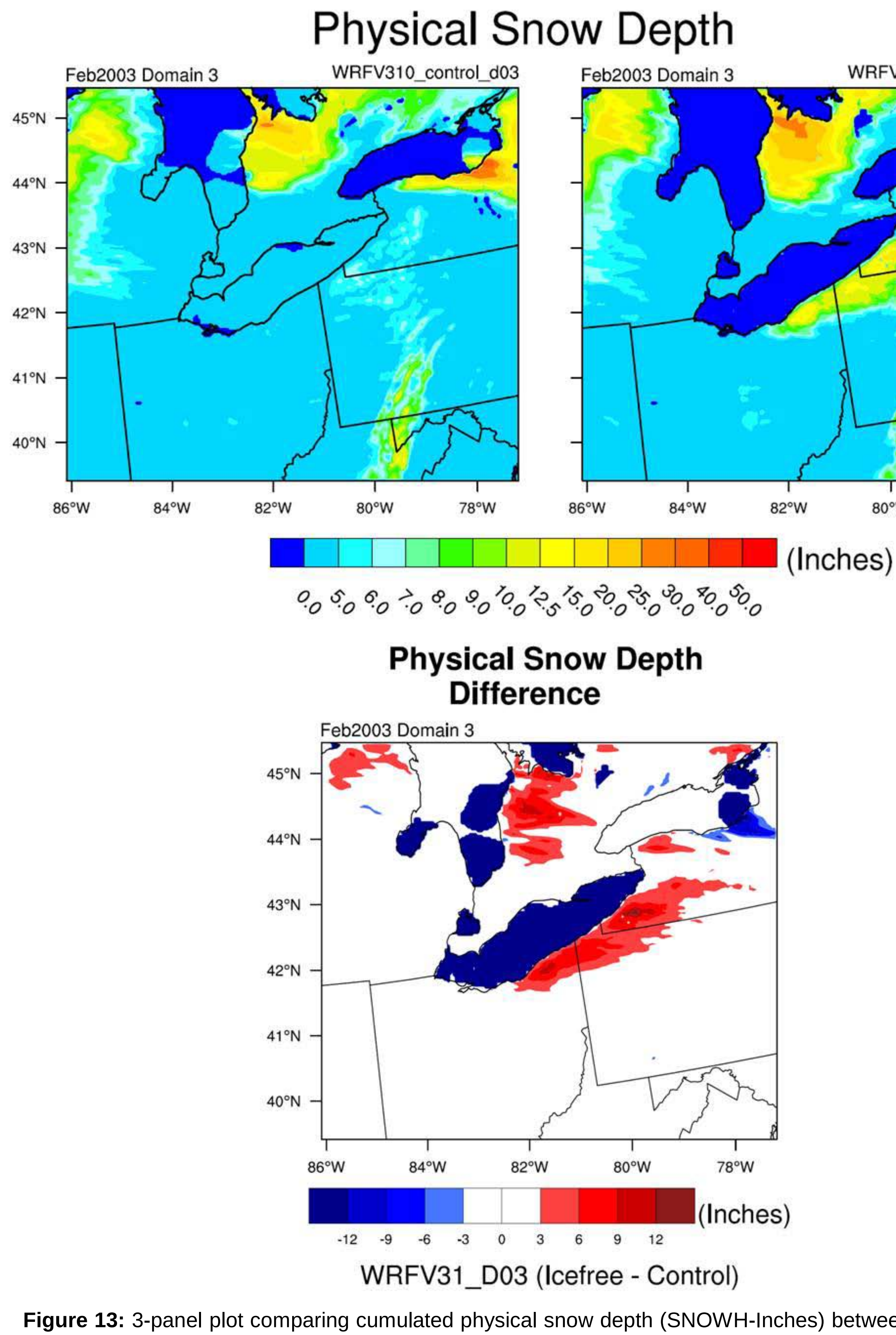

Figure 13: 3-panel plot comparing cumulated physical snow depth (SNOWH-Inches) between WRF_V31 control (top left) and the WRF_V31 ice-free case (top right) with a difference plot of the ice-free case subtracted from the control case (lower panel) as in Fig. 9.

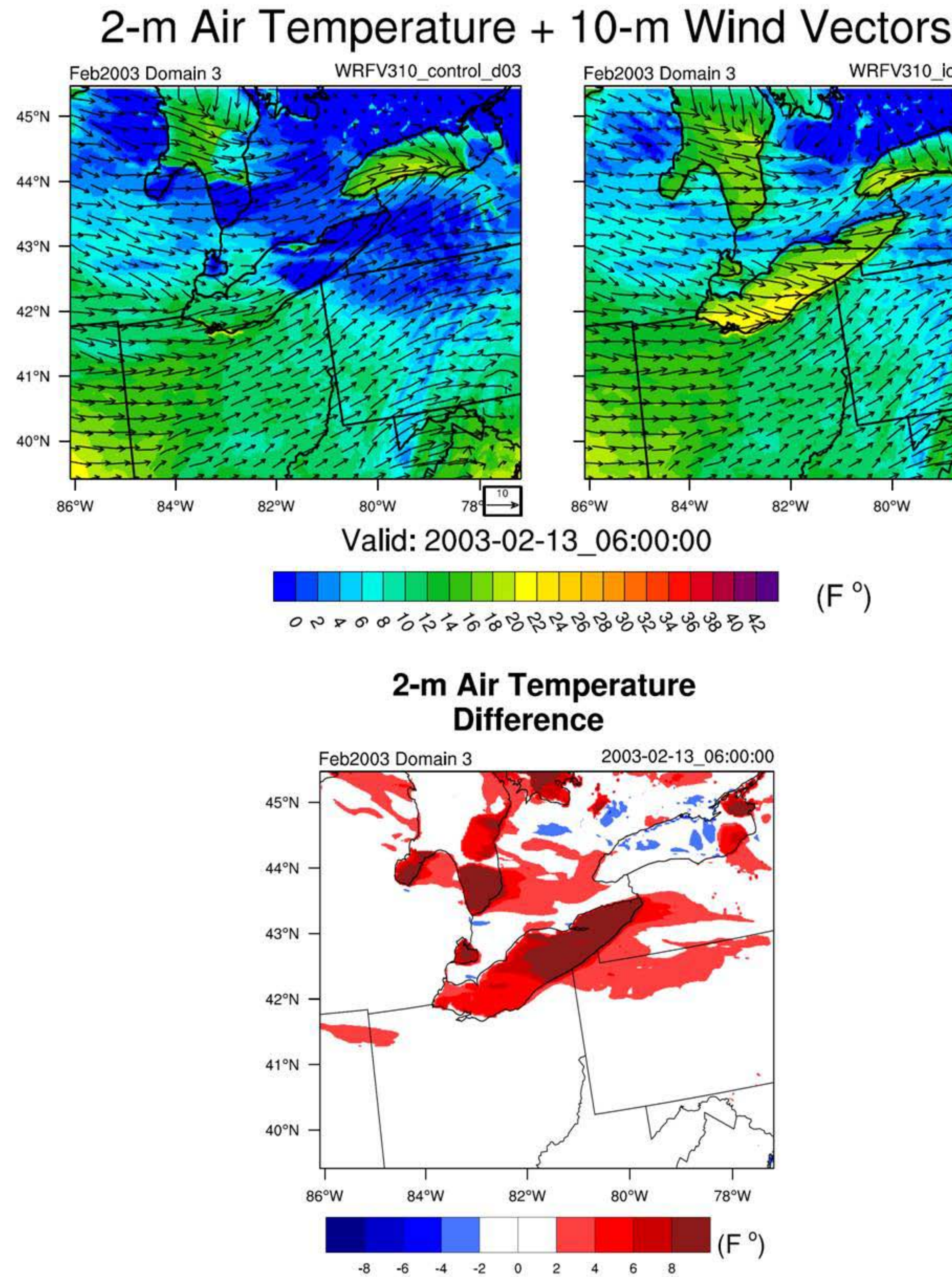

Figure 14: 3-panel plot showing 2-m air temperature (F) and 10-m wind vectors of the WRFV31_control (upper left) and WRFV31_icefree (upper right) cases 06:00 UTC 13, February 2003. The lower plot represents the difference between the ice-free case and the control case as in Fig. 9.

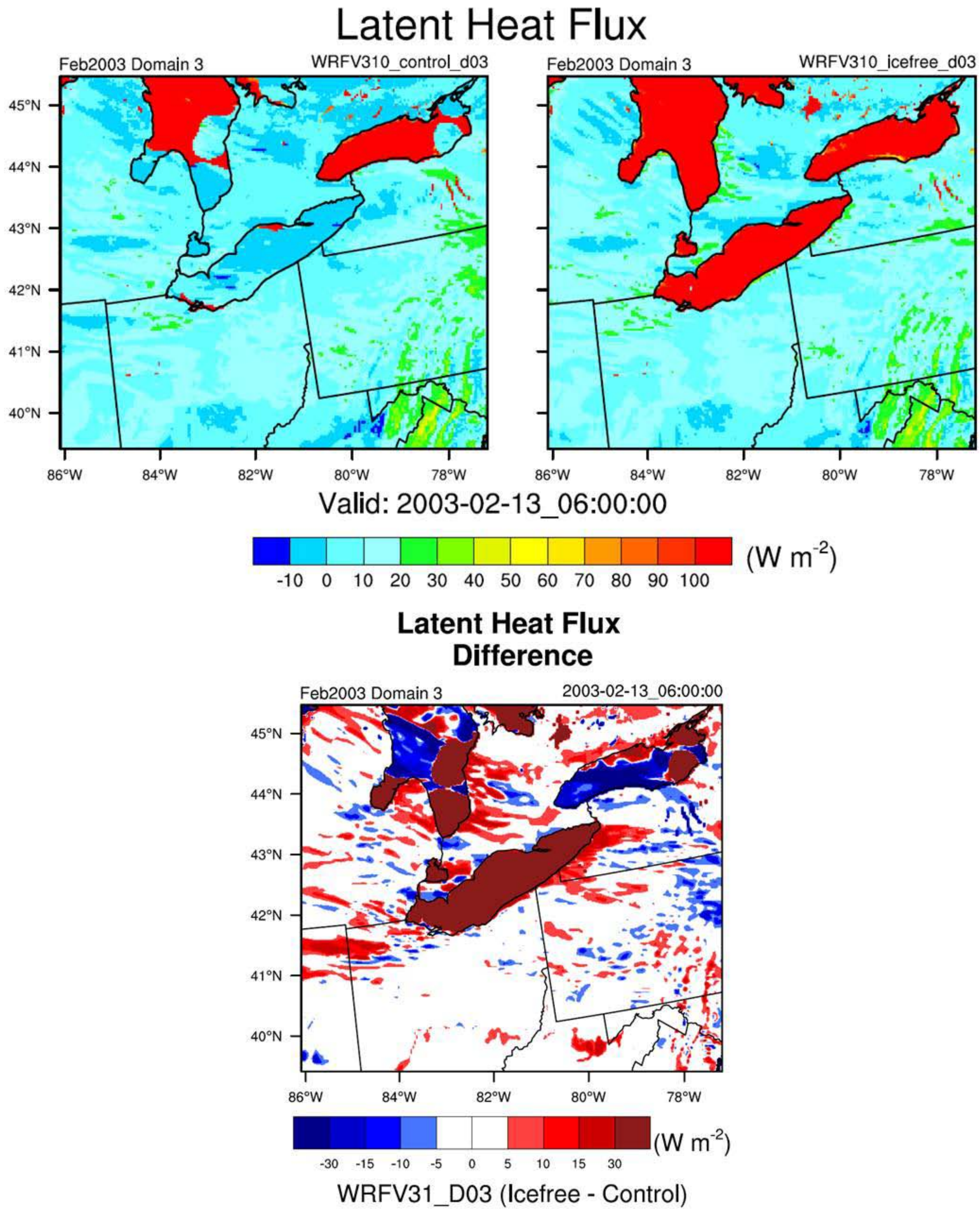

Figure 15: 3-panel plot comparing the WRFV31_control (upper left) and the WRFV31_icefree (upper right) output for latent heat flux (LH- W/m^2) for the Feb2003 Cordeira case for 06:00 UTC, 13 February, 2003. The difference between the ice-free case and the control case is illustrated in the lower panel as in Fig. 9.

4. CONCLUSION

Initial results for the Gerbush non-LE snow case show significant modifications to the environment pertaining to primary LE snow mechanisms. Temperature and moisture fields suggest that over complex ice fields, modification to both temperature and moisture fields occur and can influence the advection trends of each field by perturbing the mesoscale circulations. The results illustrate the ability of complex ice fields to influence mesoscale circulations under low wind conditions where gradients can form between open water and ice-covered regions and enhance convergence zones. Influences on convergence zones can enhance or suppress the convective boundary layer's growth, and thus the potential for LE snow accumulations. When stronger winds prevail, those gradients become mixed out and advection transports heat and moisture biases downwind of the region of fractional ice cover. Surface heat flux fields show a substantial sensitivity to ice cover where considerably larger values of both SH and LH occur over the warmer SSTs of the water body.

Initial results from the February 2003 Cordeira case showed that the removal of ice cover had a substantial influence on LE, controlling fields such as temperature/moisture and SH/LH leading to large accumulations of snowfall downwind of the Great Lakes, particularly Lake Erie. Temperature and moisture fields showed the expected biases towards warmer and more moist surface conditions anticipated over a warm open water body. In addition, the ice-free simulation resolved mesoscale convergence zones on the windward side of Lake Erie, enhancing the convective boundary layer. The ability of the ice-free case to resolve the location of largest snowfall accumulations as shown by the National Weather Service's Lake Storm Newton analysis (Fig. 8), hints at the model's ability to accurately resolve the timing and location of enhanced LE snowfall events when not being suppressed by unrealistic amounts of ice cover. Due to the amount of ice cover for the Feb. 2003 Cordeira case; it is suspected that values of snowfall accumulations or heat flux and 2-m fields would not be achieved for the high resolution ice case. Instead the natural case would fall in between the two cases compared for this section of results. As was observed and noted in Fig. 8 of the NWS analysis of snowfall totals, the maximum accumulation downwind of Lake Erie was approximately 6 inches, reasonable considering maximum accumulations from the ice-free case were between 20 and 25 inches, which occurred under ideal conditions and no ice cover.

For the case of NWP prediction of LE snowfall, the ability to accurately resolve these heat flux fields is paramount to increasing confidence in guidance products utilized by operational forecasters. As seen in the representation of the SEAICE comparisons between the default control WRF runs and the MODIS satellite derived high resolution ice WRF simulations, in some situations default ice classifications are not capable of resolving the complex nature of the ice fields. As a result, the model may underestimate the potential for LE snowfall to occur. Many times operational forecast offices utilize NWP models such as the WRF-ARW to complete regionally specific simulations such as LE snow events. When high resolution ice field initializations such as the ones employed for this study are not readily available, the ability of an operational forecaster to acknowledge the coupling of a potential LE setup with an NWP model's bias towards over-coverage of ice can improve LE forecasting. Maintaining diligence to the fact that potentially high impact weather could occur despite model guidance favoring a non-LE event can help minimize the surprise of a LE event occurring over large ice covered lakes.

Acknowledgments: The author greatly appreciates the efforts and guidance by Dr. David Bromwich and Dr. Keith Hines, developers of Polar WRF from the Polar Meteorology Group at the Ohio State University for their contributions of the Polar WRF code, as well as their guidance towards changes required in the WRF code. The author would like to thank Dr. David Kristovich for data sets obtained during the GLICAF case study. Also, comments provided by Dick Farley greatly improved the quality of this paper and are very much appreciated. This project was funded through the National Science Foundation Grant ATM-0511967, as well as the generous contributions of the Harold and Laura Orville Endowment and the Dale Hjermstad Memorial Scholarship Endowment.

References:

Bromwich, D. H., K. M. Hines, and L.S. Bai, 2009: Development and testing of Polar WRF: 2. Arctic Ocean. *J. Geophys. Res.*, **114**, D08122.

Chen, F., and J. Dudhia, 2001a: Coupling an advanced land surface-hydrology model with the Penn State-NCAR MM5 modeling system:

Part I: Model implementation and sensitivity, *Monthly Weather Review*, ***129***(4), 569-585.

Chen, F., and J. Dudhia, 2001b: Coupling an advanced land surface-hydrology model with the Penn State-NCAR MM5 modeling system: Part II: Preliminary model validation. *Mon. Wea. Rev.,* **129**, 587-604.

Cordeira, J.M., and N.F. Laird, 2008: The Influence of Ice Cover on Two Lake-Effect Snow Events over Lake Erie. *Mon. Wea. Rev*., **139**, 2747-2763.

Gerbush, M.R., D.A.R. Kristovich, and N.F. Laird, 2008: Mesoscale Boundary Layer and Heat Flux Variations over Pack Ice-Covered Lake Erie. *J. of App. Met. and Climatology*, **47**, 668-682.

Hines, K. M., and D. H. Bromwich, 2008: Development and Testing of Polar WRF. Part I. Greenland Ice Sheet Meteorology. *Mon. Wea. Rev.*, **136**, 1971-1989.

Mesinger, F., G. DiMego, E. Kalnay, K. Mitchell, P. Shafran, W. Ebisuzaki, D. Jović, J. Woolen, E. Rogers, E. H. Berbery, M. B. Ek, Y. Fan, R. Grumbine, W. Higgins, H. Li, G. Manikin, D. Parish, and W. Shi, 2006: North American Regional Reanalysis, *Bulletin of the American Meteorological Society*, ***87***(3), 343-360.

Skamarock, W. C., J. B. Klemp, J. Dudhia, D. O. Gill, D. M. Barker, M. Duda, X.-Y. Huang, W. Wang, and J. G. Powers, 2008: A description of the Advanced Research WRF Version 3, *NCAR Technical Note Rep. NCAR/TN-479+STR*, 88 pp, National Center for Atmospheric Research, Boulder, CO.